

Solution Infrared Spectroscopic Studies on Equilibrium Reactions of CO with the Decamethylmetallocenes $\text{Cp}^*_2\text{M}^{\text{II}}$, Where $\text{M}^{\text{II}} = \text{Mg, Ca, Sr, Ba, Sm, Eu, Yb}$

Peter Selg,[†] Hans H. Brintzinger,^{*,†} Madeleine Schultz,[‡] and Richard A. Andersen^{*,‡}

Fachbereich Chemie, Universität Konstanz, 78457 Konstanz, Germany, and Chemistry Department and Chemical Sciences Division of Lawrence Berkeley National Laboratory, University of California, Berkeley, California 94720

Received December 7, 2001

The reaction of CO with the alkaline-earth decamethylmetallocenes $\text{Cp}^*_2\text{M}^{\text{II}}$, where M^{II} is Mg, Ca, Sr, or Ba, and the bivalent lanthanide decamethylmetallocenes, where M^{II} is Sm, Eu, or Yb, have been studied in toluene or methylcyclohexane solution in a high-pressure infrared cell. In all cases, except for Mg and Ba, the monocarbonyl complex Cp^*_2MCO is observed to form under CO pressure. The CO stretching frequencies for Cp^*_2CaCO (2158 cm^{-1}), Cp^*_2SrCO (2159 cm^{-1}), Cp^*_2SmCO (2153 cm^{-1}), and Cp^*_2EuCO (2150 cm^{-1}) are greater than that of free CO (2134 cm^{-1} in toluene or methylcyclohexane). In contrast, Cp^*_2YbCO has ν_{CO} 2114 cm^{-1} , below that of free CO. This 1:1 complex is formed at low CO pressure (<2 bar); at higher CO pressures the 1:2 adduct $\text{Cp}^*_2\text{Yb}(\text{CO})_2$ with an even lower ν_{CO} value of 2072 cm^{-1} predominates. Equilibrium constants were determined as a function of pressure and temperature for the equilibria $\text{Cp}^*_2\text{M}^{\text{II}}(\text{solvent}) + n\text{CO}(\text{gas or solvent}) \rightleftharpoons \text{Cp}^*_2\text{M}^{\text{II}}(\text{CO})_n(\text{solvent})$, with $\text{M}^{\text{II}} = \text{Ca, Eu, Yb}$. The thermodynamic constants ΔH° , ΔS° , and ΔG° for the formation of each species, extracted from the changes in the intensity of the corresponding IR absorption bands, indicate weak $\text{M}^{\text{II}}\text{--CO}$ binding. Models to account for the bonding in these metallocene CO adducts are discussed.

Introduction

Carbon monoxide is a ubiquitous ligand for the *nd* transition metals in their lower oxidation states.¹ Carbonyl complexes have been isolated with nearly every *nd^x* electron configuration, where *n* is 3–5 and *x* is 0–10; even some cationic carbonyl cations such as $[\text{Ir}(\text{CO})_6]^{3+}$ and $[\text{Os}(\text{O})_2(\text{CO})_4]^{2+}$ have been isolated.^{2–4} In matrix isolation studies at cryogenic temperatures with the metal atoms^{5–7} or the metal trifluorides,⁸ lanthanide carbonyl complexes have been observed but not isolated.⁹ The binary lanthanide carbonyl adducts resulting from these experiments, in which the single observed CO stretching frequency is lower by 150–195 cm^{-1} than that of free CO, are assumed to be the hexacarbonyls, $\text{M}(\text{CO})_6$. In contrast, CO adducts of the matrix-isolated

lanthanide trifluoride species have stretching frequencies higher by 50–75 cm^{-1} than free CO. In a qualitative study, several ring-substituted ytterbocene derivatives have been observed to form adducts with CO in methylcyclohexane solution under 1 bar of CO, with stretching frequencies depending upon the ring substituents.¹⁰

In the 5f transition series, reaction of matrix-isolated UF_4 with CO has been studied; as in the trivalent lanthanides, ν_{CO} is found to increase by 40 cm^{-1} upon coordination.¹¹ In cryogenic matrixes a carbonyl complex with ν_{CO} 1961 cm^{-1} , assumed to be $\text{U}(\text{CO})_6$, was observed to form from uranium atoms.¹² Recently, families of binary carbonyls, $\text{U}(\text{CO})_n$ (*n* = 1–6) and $\text{Th}(\text{CO})_n$ (*n* = 1–3), with ν_{CO} shifted to lower energies, e. g. with ν_{CO} 1918 and 1818 cm^{-1} in $\text{U}(\text{CO})$ and $\text{Th}(\text{CO})$, respectively, have likewise been observed in cryogenic matrixes.^{13,14} Theory suggests that π -back-bonding due to 6d electrons is largely responsible for the formation of U–CO and Th–CO adducts. Interestingly, the average value of ν_{CO} in the bis adducts $\text{U}(\text{CO})_2$ and $\text{Th}(\text{CO})_2$, 1825 and 1806 cm^{-1} , is lower than that in the monoadducts. A trivalent uranium metallocene, $(\text{Me}_3\text{SiC}_5\text{H}_4)_3\text{U}$, yields in solution a monocarbonyl complex, $(\text{Me}_3\text{SiC}_5\text{H}_4)_3\text{U}(\text{CO})$.

[†] Universität Konstanz.

[‡] University of California.

(1) Cotton, F. A.; Wilkinson, G.; Murillo, C. A.; Bochmann, M. *Advanced Inorganic Chemistry*, 6th ed.; Wiley: New York, 1999.

(2) Bach, C.; Willner, H.; Wang, C.; Rettig, S. J.; Trotter, J.; Aubke, F. *Angew. Chem., Int. Ed. Engl.* **1996**, *35*, 1974–1976.

(3) Willner, H.; Aubke, F. *Angew. Chem., Int. Ed. Engl.* **1997**, *36*, 2402–2425.

(4) Bernhardt, E.; Wilner, H.; Jonas, V.; Thiel, W.; Aubke, F. *Angew. Chem., Int. Ed.* **2000**, *39*, 168.

(5) Slater, J. L.; DeVore, T. C.; Calder, V. *Inorg. Chem.* **1973**, *12*, 1918–1921.

(6) Slater, J. L.; DeVore, T. C.; Calder, V. *Inorg. Chem.* **1974**, *13*, 1808–1812.

(7) Sheline, R. K.; Slater, J. L. *Angew. Chem., Int. Ed. Engl.* **1975**, *14*, 309–313.

(8) Hauge, R. H.; Gransden, S. E.; Margrave, J. L. *J. Chem. Soc., Dalton Trans.* **1979**, 745–748.

(9) Ellis, J. E.; Beck, W. *Angew. Chem., Int. Ed. Engl.* **1995**, *34*, 2489–2491.

(10) Schultz, M.; Burns, C. J.; Schwartz, D. J.; Andersen, R. A. *Organometallics* **2001**, *20*, 5690–5699.

(11) Kunze, K. R.; Hauge, R. H.; Hamill, D.; Margrave, J. L. *J. Phys. Chem.* **1977**, *81*, 1664–1667.

(12) Slater, J. L.; Sheline, R. K.; Lin, K. C.; Weltner, W. *J. Chem. Phys.* **1971**, *55*, 5129–5130.

(13) Zhou, M.; Andrews, L.; Li, J.; Bursten, B. E. *J. Am. Chem. Soc.* **1999**, *121*, 9712–9721.

(14) Li, J.; Bursten, B. E.; Zhou, M.; Andrews, L. *Inorg. Chem.* **2001**, *40*, 5448.

$\text{SiC}_5\text{H}_4)_3\text{U}(\text{CO})$, with ν_{CO} 1976 cm^{-1} , which cannot be isolated.^{15,16} In the isolated complex $(\text{Me}_4\text{C}_5\text{H})_3\text{U}(\text{CO})$, ν_{CO} is 1900 cm^{-1} and a single-crystal X-ray crystallographic study shows that the carbon monoxide is linear and carbon-bound.¹⁷ In contrast, no CO binding is observed for base-free trivalent lanthanide metallocenes $(\text{Me}_3\text{SiC}_5\text{H}_4)_3\text{M}$, $\text{M} = \text{Ce}, \text{Nd}$ under similar conditions.¹⁶

The s- and p-block metals and their compounds do form adducts with CO, but, like the 4f-block metal complexes, the existence of the carbonyls is inferred from infrared spectroscopy only. Borane carbonyl, H_3BCO , which was isolated over 60 years ago, is a notable exception.^{18,19} Its ν_{CO} value of 2165 cm^{-1} is greater than that of free CO, and the structure in the gas phase shows that carbon monoxide is carbon-bound. Trimethylaluminum forms a CO adduct with ν_{CO} 2185 cm^{-1} in a CO matrix at cryogenic temperatures; at room temperature, no coordination was observed at pressures up to 10 bar.²⁰ The bivalent silicon species Me_2Si and Cp^*_2Si were found in low-temperature experiments to coordinate CO with stretching frequencies of 1962 and 2065 cm^{-1} , respectively.^{21–23} A CO complex of the s-metal complex $n\text{-BuLi}$, with ν_{CO} 2047 cm^{-1} , has been detected at -100 °C in supercritical xenon.²⁴ In a preliminary study, the molecular s-block metallocene Cp^*_2Ca has been found to give a CO adduct with ν_{CO} 2158 cm^{-1} .²⁵

The a priori unexpected tendency of the decamethylmetallocenes Cp^*_2Ca and Cp^*_2Yb to coordinate CO has led us to investigate more systematically CO complex formation reactions of permethylmetallocenes containing bivalent metals of the alkaline-earth and lanthanide series.

Due to their solubility in hydrocarbon solvents, these complexes are particularly suitable for investigating reversible interactions with CO. In this paper, we present results of quantitative studies on equilibrium reactions between carbon monoxide and the alkaline-earth and bivalent lanthanide metallocenes $\text{Cp}^*_2\text{M}^{\text{II}}$, where M^{II} is Ca, Eu, and Yb, and qualitative information on those where M^{II} is Mg, Sr, Ba, and Sm.

Results and Discussion

Cp^*_2Ca . When a solution of Cp^*_2Ca in toluene is exposed to CO pressures of 2–60 bar in an elevated-pressure infrared cell, a new CO stretching band appears in the IR spectrum at a frequency of 2158 cm^{-1}

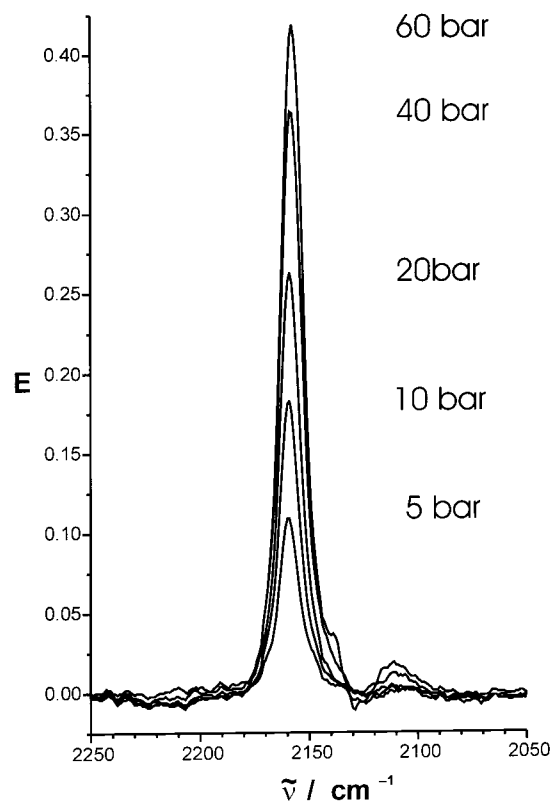
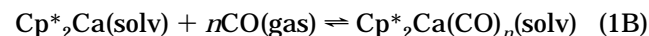
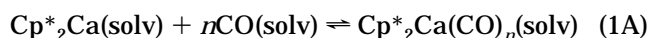


Figure 1. Infrared spectrum of a 0.04 M solution of Cp^*_2Ca in toluene at 10 °C and CO pressures of 5–60 bar, corrected for background, solvent, and free CO absorptivities.

(Figure 1). At each temperature, the intensity of the band at 2158 cm^{-1} increases with increasing CO pressure and approaches saturation at higher CO pressures (Figure 2). This and the disappearance of the band at 2158 cm^{-1} upon release of the CO pressure indicate a system in chemical equilibrium. The band at 2158 cm^{-1} is likely to be due to a carbonyl complex of the type $\text{Cp}^*_2\text{-Ca}(\text{CO})_n$, formed in the equilibrium $\text{Cp}^*_2\text{Ca} + n\text{CO} \rightleftharpoons \text{Cp}^*_2\text{Ca}(\text{CO})_n$.

Depending on whether complex formation is determined as a function of CO concentrations or CO pressures, the equilibrium can be written either as in eq 1A or as in eq 1B. These equilibrium expressions are interconvertible by use of the proportionality between $[\text{CO}]$ in toluene and P_{CO} (eq 2), found to be valid, independent of the temperature, in the temperature and pressure range used.^{26–28}



$$[\text{CO}] = 0.0071P_{\text{CO}} \quad (2)$$

Two quantities are defined by the equilibrium reaction in eqs 1A and 1B, viz., n , the number of CO groups

(26) Because of the relation $K_C = K_p/0.0071$, ΔS° must be more negative by $R \ln(1/0.0071) = 41$ J/(mol K) for eq 1A, which refers to a standard state of $[\text{CO}] = 1$ mol/L, than for eq 1B, which refers to a standard state of $P_{\text{CO}} = 101.3$ kPa, while the experimentally determined values of ΔF° are unaffected by the choice of standard states.

(27) van Raaij, E. U.; Schmulbach, C. D.; Brintzinger, H. H. *J. Organomet. Chem.* **1987**, *328*, 275–285. van Raaij, E. U. Dissertation, University of Konstanz, Konstanz, 1989.

(28) van Raaij, E. U.; Brintzinger, H. H. *J. Organomet. Chem.* **1988**, *356*, 315–323.

(15) Brennan, J. G.; Andersen, R. A.; Robbins, J. L. *J. Am. Chem. Soc.* **1986**, *108*, 335–336.

(16) del Mar Conejo, M.; Parry, J. S.; Carmona, E.; Schultz, M.; Brennan, J. B.; Beshouri, S. M.; Andersen, R. A.; Rogers, R. D.; Coles, S.; Hursthouse, M. *Chem. Eur. J.* **1999**, *5*, 3000–3009.

(17) Parry, J.; Carmona, E.; Coles, S.; Hursthouse, M. *J. Am. Chem. Soc.* **1995**, *117*, 2649–2650.

(18) Burg, A. B.; Schlesinger, H. I. *J. Am. Chem. Soc.* **1937**, *59*, 780–787.

(19) Gordy, W.; Ring, H.; Burg, A. B. *Phys. Rev.* **1950**, *78*, 512–517.

(20) Sanchez, R.; Arrington, C.; Arrington, C. A. *J. Am. Chem. Soc.* **1989**, *111*, 9110–9111.

(21) Arrington, C. A.; Petty, J. T.; Payne, S. E.; Haskins, W. C. K. *J. Am. Chem. Soc.* **1988**, *110*, 6240–6241.

(22) Pearsall, M.-A.; West, R. *J. Am. Chem. Soc.* **1988**, *110*, 7228–7229.

(23) Tacke, M.; Klein, C.; Stufkens, D. J.; Oskam, A.; Jutzi, P.; Bunte, E. A. *Z. Anorg. Allg. Chem.* **1993**, *619*, 865–868.

(24) Tacke, M. *Chem. Ber.* **1995**, *128*, 1051–1053.

(25) Selg, P.; Brintzinger, H. H.; Andersen, R. A.; Horvath, I. T. *Angew. Chem., Int. Ed. Engl.* **1995**, *34*, 791–793. Selg, P. Dissertation, Universität Konstanz, 1996.

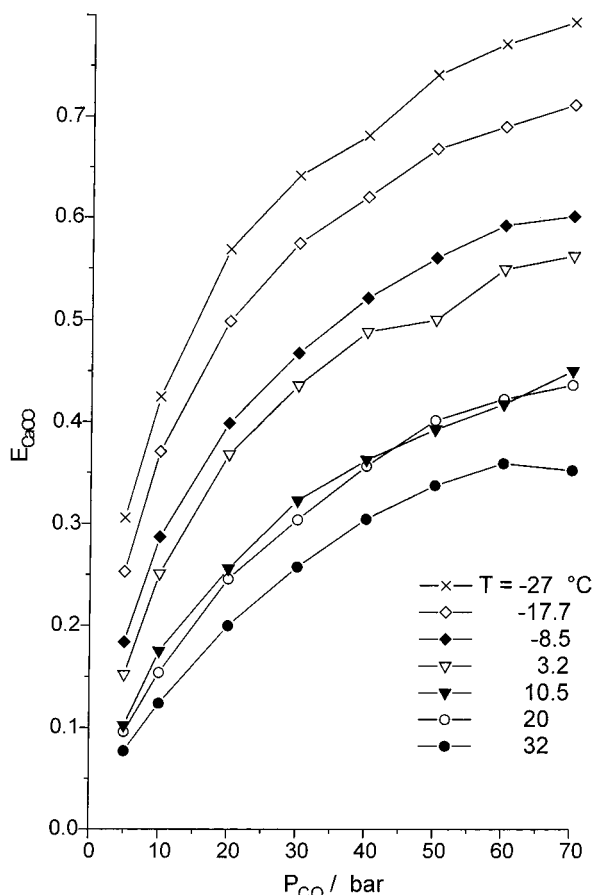


Figure 2. Absorptivity of $\text{Cp}^*_2\text{Ca}(\text{CO})_n$ in toluene as a function of CO pressure at temperatures from -27 to $+32$ °C.

bonded to the metallocene, and K_C and K_P , as defined by eqs 3A and 3B, respectively, where $\{\text{Ca}\} = \text{Cp}^*_2\text{Ca}$. On the basis of eq 2, K_C and K_P are related by $K_C = K_P/(0.0071)^n$.

$$K_C = \{[\text{Ca}]\text{CO}\}_n \{[\text{Ca}][\text{CO}]^n\}^{-1} \quad (3A)$$

$$K_P = \{[\text{Ca}]\text{CO}\}_n \{[\text{Ca}](P_{\text{CO}})^n\}^{-1} \quad (3B)$$

The values of K_C and K_P can be obtained from the dependence on CO concentrations and pressures, respectively, of the absorptivity E_{CaCO} of the complex $\text{Cp}^*_2\text{Ca}(\text{CO})_n$ by use of the appropriate form of the Hildebrand–Benesi equation (eq 4A or 4B),²⁹ where $Z = \{[\text{Ca}]\}_{\text{TOT}} \epsilon_{\text{CaCO}} d$, with $\{[\text{Ca}]\}_{\text{TOT}}$ being the total calcocene concentration, ϵ_{CaCO} the molar extinction coefficient of $\text{Cp}^*_2\text{Ca}(\text{CO})_n$, and d the path length of the infrared cell.

$$1/E_{\text{CaCO}} = (ZK_C)^{-1}[\text{CO}]^{-n} + 1/Z \quad (4A)$$

$$1/E_{\text{CaCO}} = (ZK_P)^{-1}(P_{\text{CO}})^{-n} + 1/Z \quad (4B)$$

Plotting $1/E_{\text{CaCO}}$ vs $(P_{\text{CO}})^{-n}$ is expected to give a straight line with slope $(ZK_P)^{-1}$ and intercept $1/Z$. To determine the value of n , $1/E_{\text{CaCO}}$ vs $(P_{\text{CO}})^{-n}$ is plotted for various integral values of n . The plot with the best linear fit yields the stoichiometric coefficient n of CO in eq 1. Plots of this kind (Figure 3) show a close

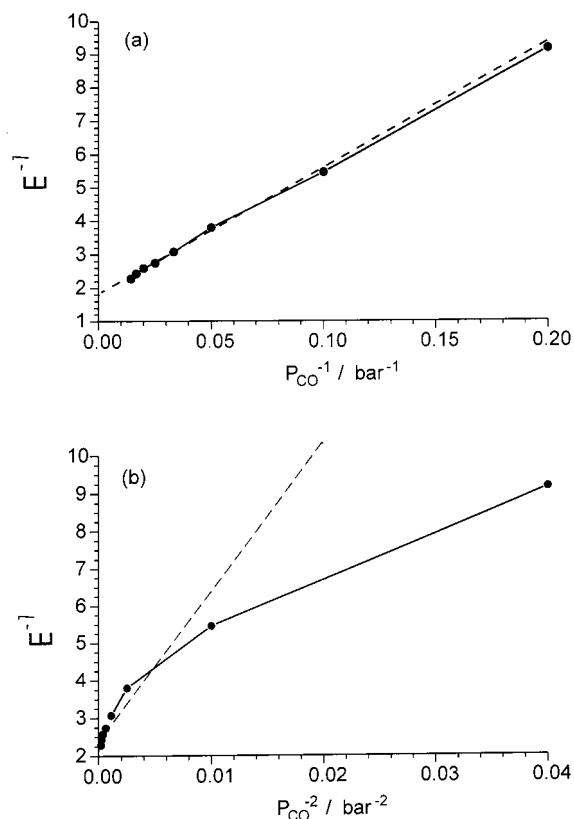


Figure 3. Hildebrand–Benesi plots for $\text{Cp}^*_2\text{Ca}(\text{CO})_n$ for $n = 1$ (a, top) and $n = 2$ (b, bottom) at 10 °C in toluene. The dotted line in each plot is the line of best fit.

linearity of the graph for $n = 1$, while the graph for $n = 2$ is clearly not an appropriate description of the experimental data. The stoichiometry of the carbonyl complex of decamethylcalcocene, giving rise to the infrared band at 2158 cm^{-1} in toluene solution, is thus certainly that of the monocarbonyl species $\text{Cp}^*_2\text{Ca}(\text{CO})$.

Analysis of the data represented in Figure 2 by use of the Benesi–Hildebrand equation (eqs 4A and 4B) with $n = 1$ gives values of K_C in units of M^{-1} and of K_P in units of bar^{-1} , as a function of temperature in the range -27 to $+32$ °C.³⁰ From van't Hoff plots of $\ln K_C$ or $\ln K_P$ vs $1/T$, the standard enthalpy and entropy changes are determined for the complex formation reactions (1A) and (1B) in toluene solution. Thermodynamic parameters for the reactions (1A) and (1B) are listed in Table 1 along with values for K_C and K_P and for the standard free energy changes ΔG°_C and ΔG°_P at 20 °C, derived from the respective K values.³⁰

To check the accuracy of the equilibrium constants deduced from the infrared spectra, a high-pressure $^{13}\text{C}\{-^1\text{H}\}$ NMR spectroscopic method was developed.²⁵ The equilibrium constant at 20 °C in $\text{tol-}d_8$ was estimated to be $K_C = 3.5 \pm 0.7 \text{ M}^{-1}$, in acceptable agreement with the value of $4.9 \pm 0.1 \text{ M}^{-1}$ obtained by the IR method. Volumetric gas uptake studies in toluene as a function of temperatures in the range of -40 to $+30$ °C, done in a manner similar to that reported for the reaction between Cp_2Cr and CO ,³¹ gave values of $\Delta H^\circ = -19 \pm 1 \text{ kJ mol}^{-1}$ and $\Delta S^\circ_P = -82 \pm 3 \text{ J/(mol K)}$ for the

(29) Benesi, H. A.; Hildebrand, J. H. *J. Am. Chem. Soc.* **1949**, *71*, 2703–2707.

(30) See the Supporting Information.
(31) Wong, K. L. T.; Brintzinger, H. H. *J. Am. Chem. Soc.* **1975**, *97*, 5143–5146.

Table 1. Thermodynamic Data for the Reactions of Cp*₂M^{II} (M^{II} = Ca, Eu, Yb) and Cp*₂Yb(CO) with CO, Calculated from Infrared Intensities

system ({M} = Cp* ₂ M ^{II})	state of CO	ν_{CO} (cm ⁻¹)	solvent	K_{P} or K_{C} at 20 °C	ΔH° (kJ mol ⁻¹)	ΔS° (J mol ⁻¹ K ⁻¹)	$\Delta G^{\circ}_{\text{C}}$ or $\Delta G^{\circ}_{\text{P}}$ (kJ mol ⁻¹) at 20 °C
{Ca} + CO	gas	2158	toluene	0.035(1) bar ⁻¹	-17.1 ± 1.9	-85.2 ± 6.8	+7.9 ± 1.6
	soln		toluene	4.9(1) M ⁻¹	-17.1 ± 1.9	-44.1 ± 6.8	-4.2 ± 1.1
{Eu} + CO	gas	2150	MCH	0.020(1) bar ⁻¹	-19.8 ± 2.2	-101.1 ± 7.9	+9.8 ± 1.9
	soln		MCH	2.0(1) M ⁻¹	-20.5 ± 1.7	-65.8 ± 6.0	-1.2 ± 0.2
{Yb} + CO	gas	2114	MCH	0.34(1) bar ⁻¹	-7.3 ± 0.7	-34.1 ± 2.3	+2.7 ± 0.5
	soln		MCH	34(6) M ⁻¹	-7.3 ± 0.7	+4.4 ± 2.1	-8.6 ± 4.8
{Yb}(CO) + CO	gas	2072	MCH	0.66(3) bar ⁻¹	-43.1 ± 2.4	-150 ± 8	+1.1 ± 0.2
	soln		MCH	67(3) M ⁻¹	-42.9 ± 1.8	-111 ± 6	-10.4 ± 0.9

reaction (1A), in good agreement with those found by the IR method (Table 1). The thermodynamic data obtained for the complex formation between Cp*₂Ca and CO can thus be considered reasonably reliable. The standard enthalpy change of $\Delta H^{\circ} = -17 \pm 2$ kJ/mol points to a rather weak bond between Cp*₂Ca and CO, while the standard entropy change of $\Delta S^{\circ}_{\text{P}} = -83 \pm 2$ J/(mol K) is in accord with expectations for a reaction which consumes 1 mol of gas.

To assess possible interferences of metal–toluene interactions with CO uptake equilibria, analogous measurements of the equilibrium constant according to eq 3A were performed also in methylcyclohexane (MCH) instead of toluene as solvent. Although the data thus obtained are generally less accurate than those described above for toluene solutions, due to decreased solubility of Cp*₂Ca and to difficulties in subtracting background absorptions, a value of $K_{\text{C}} \approx 4.8 \pm 0.7$ M⁻¹, obtained in MCH solution at 20 °C, is practically equal to that determined in toluene solution and would thus indicate that solvent interactions with Cp*₂Ca do not significantly affect the CO uptake equilibria.

Cp*₂Mg, Cp*₂Sr, and Cp*₂Ba. These alkaline-earth metallocenes were examined only in a qualitative fashion by infrared spectroscopy. For Cp*₂Mg in toluene, no carbonyl absorption due to adduct formation was observed up to pressures of 50 bar. The infrared spectrum of Cp*₂Sr in methylcyclohexane (MCH) develops a new carbonyl stretching band at 2158 cm⁻¹ under CO pressures of 10–60 bar, which disappears when the pressure is released.³⁰ The intensity of the ν_{CO} absorption band increases with CO pressure, but the absorptivity changes are much smaller than those observed in the case of Cp*₂Ca. The equilibrium constant $K_{\text{C}} = 0.003$ bar⁻¹ at 298 K is estimated for the formation of Cp*₂SrCO, but the errors for K_{C} at other temperatures are too large for a determination of thermodynamic quantities to be feasible. For Cp*₂Ba in toluene, any increase of absorptivity between 2140 and 2170 cm⁻¹ is too small for any equilibrium studies or even for a reliable estimate of ν_{CO} from the absorption maximum.

Cp*₂Sm. Due to their tendency to decompose in toluene solution under CO during the course of the IR experiments, all of the bivalent lanthanide metallocenes had to be measured in methylcyclohexane (MCH) as a solvent, even though their solubilities in MCH were smaller than in toluene. The behavior of Cp*₂Sm in MCH solution is similar to that of Cp*₂Sr. An absorption band at ν_{CO} 2153 cm⁻¹ is observed under CO, but the intensity changes with CO pressure are too small to provide accurate equilibrium constants.³⁰ Nevertheless,

the reaction is reversible; the metallocene can be crystallized unchanged after releasing CO pressure. The THF complex Cp*₂Sm(THF)₂ does not give rise to any IR band other than that of free CO in MCH at CO pressures of up to 70 bar.³² Apparently, CO cannot compete with THF for Cp*₂Sm.

Cp*₂Eu. Upon exposure of a methylcyclohexane solution of Cp*₂Eu to CO pressures of 2.5–40 bar, a new CO band appears at 2150 cm⁻¹. This absorption band grows in intensity as a function of the CO pressure.³⁰ Hildebrand–Benesi plots show that the value of n is 1; the molecular species giving rise to the 2150 cm⁻¹ band thus is the monocarbonyl Cp*₂EuCO. The complex formation constant K_{P} at 20 °C is given in Table 1, as are the values of ΔH° and ΔS° . The latter is in accord, again, with a reaction product which has the 1:1 stoichiometry Cp*₂EuCO.³⁰

Cp*₂Yb. The behavior of Cp*₂Yb with CO in MCH is different from that of the other metallocenes described above (see Figure 4). The spectrum at 1 bar of CO pressure is qualitatively the same as previously reported.¹⁰ Two differences between these spectra and those of Cp*₂Eu and Cp*₂Ca under the same conditions are immediately apparent; two absorption bands rather than one are observed at pressures of 1 bar and higher, and both values of ν_{CO} are lower than that found for free CO. At subatmospheric pressure, a single absorption at 2114 cm⁻¹ is the only feature that is visible. Increasing the pressure to 2.5 bar causes the absorption at 2114 cm⁻¹ to increase in intensity, along with the appearance of a broader feature at 2072 cm⁻¹. As the pressure is further increased, the absorption at 2072 cm⁻¹ increases in intensity much more rapidly than that at 2114 cm⁻¹ until it dominates at pressures greater than about 30 bar. Figure 5 shows the relative proportions of the two species as a function of pressure at 20 °C and at 60 °C.³⁴

(32) This observation conflicts with a prior publication: in 1985 Evans and co-workers³³ reported that exposure of Cp*₂Sm(THF)₂ in THF to CO at 90 psi (ca. 6 bar) for 3 days gave a brown solution from which crystals of (Cp*₂Sm)₂(THF)(C₃O₃) were isolated in 20% yield. X-ray crystallographic analysis showed that the C₃O₃ unit is the ketene–carboxy dianion O₂CC₂O²⁻, coordinated to a Cp*₂Sm and a Cp*₂Sm(THF)⁺ fragment. To verify these results, we repeated our studies in the infrared cell using tetrahydrofuran instead of MCH as solvent for reaction times of several days: i.e., under experimental conditions similar to those used in ref 33. Under these conditions, we observed no IR absorption band other than that of free CO, with 99.999% CO, no evidence for CO coordination or rearrangement is observed. When 99.99% CO was bubbled through a solution of Cp*₂Sm under N₂ in MCH, the solution immediately became green-blue and then slowly turned brown; no pure product could be crystallized from it. The experimental conditions thus appear crucial to avoid decomposition. We have to conclude that the compound isolated by Evans et al. does not result from reaction with CO alone.

(33) Evans, W. J.; Grate, J. W.; Hughes, L. A.; Zhang, H.; Atwood, J. L. *J. Am. Chem. Soc.* **1985**, *107*, 3728–3730.

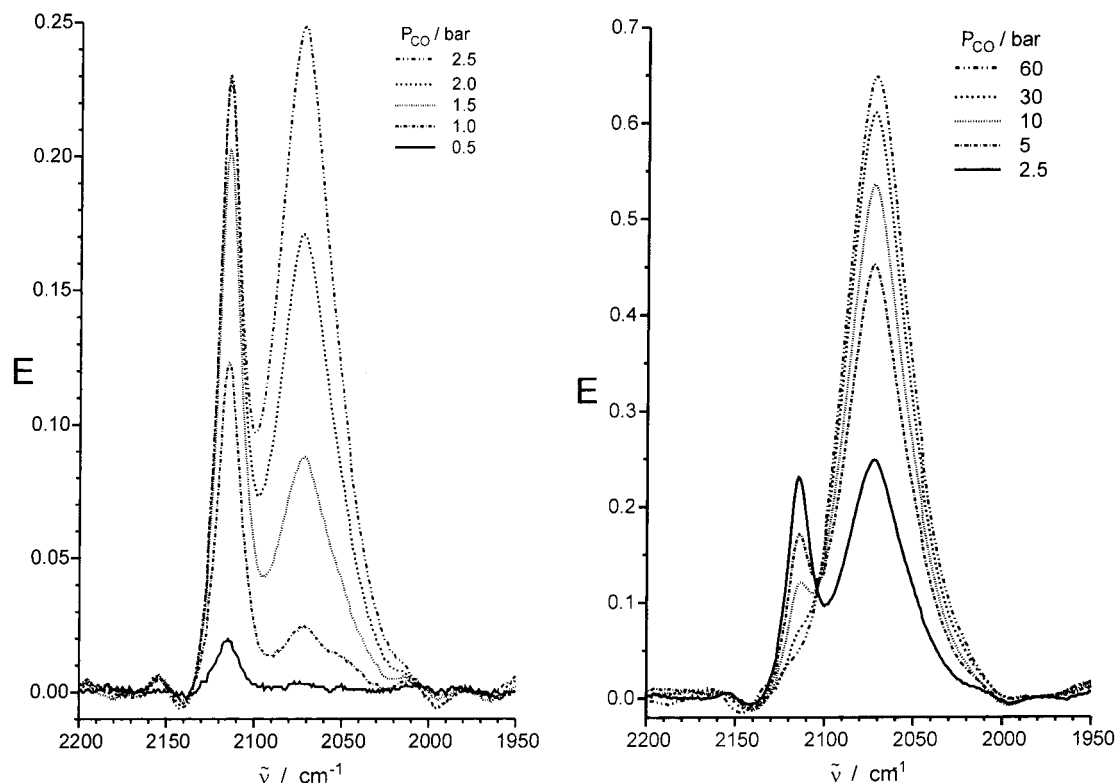
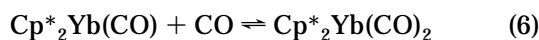
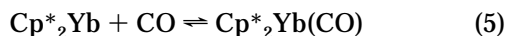


Figure 4. Infrared spectra of a 0.02 M solution of Cp^*_2Yb in MCH at 21 °C at CO from 0.5 to 2.5 bar (left) and from 2.5 to 60 bar (right), corrected for background, solvent, and free CO.

As for the other metallocenes described in this paper, the changes with pressure and temperature are reversible over at least two cycles. In the ytterbocene case, the observations are reproducible over a period of several years, implying that the experimental observations are not in doubt. Thus, at a minimum, two carbonyl-containing species are formed with decamethylytterbocene, both of which have ν_{CO} stretching frequencies below that of free CO. The simplest explanation for the two ν_{CO} stretching frequencies is that the feature at 2114 cm^{-1} is due to a monocarbonyl, $\text{Cp}^*_2\text{Yb}(\text{CO})$, and that at 2072 cm^{-1} to a dicarbonyl, $\text{Cp}^*_2\text{Yb}(\text{CO})_2$ (eqs 5 and 6). Reactions according to eqs 5 and 6 are supported by quantitative CO gas uptake experiments, which show that a solution of Cp^*_2Yb at -45 °C absorbs 1.73 mol of CO/mol of Cp^*_2Yb .³⁵



For both the mono- and dicarbonyl species idealized C_{2v} symmetry would be expected, as has been found for group 6 metallocene mono- and dicarbonyl species.^{27,28,31} Thus, one IR-active CO stretching vibration is expected for the monocarbonyl and two are expected for the

dicarbonyl. Only one feature is observed for the proposed dicarbonyl species, but the 2072 cm^{-1} absorption band is approximately twice as broad as the 2114 cm^{-1} absorption band. The appearance of a single, broad absorption for $\text{Cp}^*_2\text{Yb}(\text{CO})_2$ can be rationalized in a fashion similar to related observations on bis(isocyanide) complexes of the type $\text{Cp}^*_2\text{Yb}(\text{CNR})_2$,³⁶ which implies minimal mechanical and electronic coupling between the two CO vibrators through the metal fragment. Since the asymmetric and symmetric stretching vibrations will then be close in energy, a broadened, unresolved absorption band such as that observed at 2072 cm^{-1} is likely to result.

Successive CO uptake equilibria as in eqs 5 and 6 are qualitatively consistent with the intensity changes of the infrared absorptions as a function of pressure and temperature. At low pressure, the band at 2114 cm^{-1} dominates; raising the CO pressure increases the intensity of the 2072 cm^{-1} absorption at the expense of that at 2114 cm^{-1} (Figures 4 and 5). A quantitative determination of the two equilibrium constants in the $\text{Cp}^*_2\text{Yb}/\text{CO}$ reaction is more difficult, however, than in the reactions of the calcium and europium analogues, since both the mono- and dicarbonyls are present at intermediate values of pressure. To extract individual absorptivities and equilibrium constants from the changes in absorptivities at 2114 and 2072 cm^{-1} , the following approach was adopted: The stepwise complex

(34) Increasing the temperature from 21 to 60 °C at constant pressure of 60 bar (at which pressure the 2114 cm^{-1} band is no longer observed) results in a decrease in intensity of the 2072 cm^{-1} absorption (cf. Figure 5) but has little effect on the position of the band maximum.

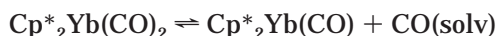
(35) This represents the maximum CO uptake. At lower temperatures, part of the Cp^*_2Yb is apparently precipitated from solution and thus not available for CO uptake; at higher temperatures, CO is lost under partial formation of the monocarbonyl complex.

(36) For related ytterbocene complexes with isocyanide ligands, only a single sharp absorption is observed in solution and in the solid state for complexes which are shown by X-ray studies to contain two isocyanide ligands bound to the metal center.¹⁰ For those complexes, the two isocyanide ligands apparently behave as independent dipoles, giving rise to a single ν_{CN} stretch.

dissociation equilibria and equilibrium constants, with $\{\text{Yb}\} = \text{Cp}^*_2\text{Yb}$, are



$$K^{\text{D}}_{\text{C}_1} = \frac{[\{\text{Yb}\}][\text{CO}]}{[\{\text{Yb}\}(\text{CO})]} \quad (8)$$



$$K^{\text{D}}_{\text{C}_2} = \frac{[\{\text{Yb}\}(\text{CO})][\text{CO}]}{[\{\text{Yb}\}(\text{CO})_2]} \quad (9)$$

The ratio of $[\text{Cp}^*_2\text{Yb}(\text{CO})]$ to the total Cp^*_2Yb concentration is shown in eq 9, where E_1 is the absorptivity of the 2114 cm^{-1} band and A_1 is the maximum value of E_1 , which would correspond to all ytterbocene present as $\text{Cp}^*_2\text{Yb}(\text{CO})$. Similarly, eq 10 can be written to give the ratio of $\text{Cp}^*_2\text{Yb}(\text{CO})_2$ to the total Cp^*_2Yb concentration. In this case, A_2 is the maximum value of E_2 , which corresponds to all ytterbium present as $\text{Cp}^*_2\text{Yb}(\text{CO})_2$. These equations can be transformed, by use of eqs 7 and 8, to eqs 11 and 12. The ratio $Q = E_1/E_2$ can thus be given by eq 13, while the sum $\Sigma E = E_1 + E_2$ is given by eq 14.

$$\frac{[\{\text{Yb}\}(\text{CO})]}{[\{\text{Yb}\}]_{\text{TOT}}} = \frac{[\{\text{Yb}\}(\text{CO})]}{[\{\text{Yb}\}] + [\{\text{Yb}\}(\text{CO})] + [\{\text{Yb}\}(\text{CO})_2]} = \frac{E_1/A_1}{1 + E_1/A_1 + E_2/A_2} \quad (9)$$

$$\frac{[\{\text{Yb}\}(\text{CO})_2]}{[\{\text{Yb}\}]_{\text{TOT}}} = \frac{[\{\text{Yb}\}(\text{CO})_2]}{[\{\text{Yb}\}] + [\{\text{Yb}\}(\text{CO})] + [\{\text{Yb}\}(\text{CO})_2]} = \frac{E_2/A_2}{1 + E_1/A_1 + E_2/A_2} \quad (10)$$

$$E_1 = A_1 K^{\text{D}}_{\text{C}_2} [\text{CO}] \{ K^{\text{D}}_{\text{C}_2} [\text{CO}] + K^{\text{D}}_{\text{C}_1} K^{\text{D}}_{\text{C}_2} + [\text{CO}]^2 \}^{-1} \quad (11)$$

$$E_2 = A_2 [\text{CO}]^2 \{ K^{\text{D}}_{\text{C}_2} [\text{CO}] + K^{\text{D}}_{\text{C}_1} K^{\text{D}}_{\text{C}_2} + [\text{CO}]^2 \}^{-1} \quad (12)$$

$$Q = E_2/E_1 = [\text{CO}] A_2 (A_1 K^{\text{D}}_{\text{C}_2})^{-1} \quad (13)$$

$$\Sigma E = E_1 + E_2 = \frac{A_1 K^{\text{D}}_{\text{C}_2} [\text{CO}] + A_2 [\text{CO}]^2}{K^{\text{D}}_{\text{C}_2} [\text{CO}] + K^{\text{D}}_{\text{C}_1} K^{\text{D}}_{\text{C}_2} + [\text{CO}]^2} \quad (14)$$

To solve this system of equations with the available physical measurements, some approximation is required. From a plot of the sum of the absorptivities, $\Sigma E = E_1 + E_2$, against P_{CO} it is apparent that ΣE reaches a constant value for values of $P_{\text{CO}} > 10$ bar (Figure 6), even though E_1 and E_2 individually still change considerably (cf. Figure 5). This must mean that upon conversion of a monocarbonyl to a dicarbonyl the loss of E_1 just compensates the gain in E_2 : i.e., that A_1 is fortuitously just equal to A_2 . Using this approximation, $A_1 \approx A_2 = A$, eqs 13 and 14 can be simplified to eqs 15 and 16.

$$Q = E_2/E_1 = [\text{CO}] (K^{\text{D}}_{\text{C}_2})^{-1} \quad (15)$$

$$\Sigma E = E_1 + E_2 = A \frac{K^{\text{D}}_{\text{C}_2} [\text{CO}] + [\text{CO}]^2}{K^{\text{D}}_{\text{C}_2} [\text{CO}] + K^{\text{D}}_{\text{C}_1} K^{\text{D}}_{\text{C}_2} + [\text{CO}]^2} \quad (16)$$

From the slope of a plot of E_2/E_1 as a function of pressure, values for $K^{\text{D}}_{\text{C}_2}$ can now be estimated for temperatures from 20 to 60 °C. Table 2 lists the corresponding association constants $K^{\text{A}}_{\text{C}_2}$. Values for $K^{\text{D}}_{\text{C}_1}$ can be obtained from the limiting values of ΣE for

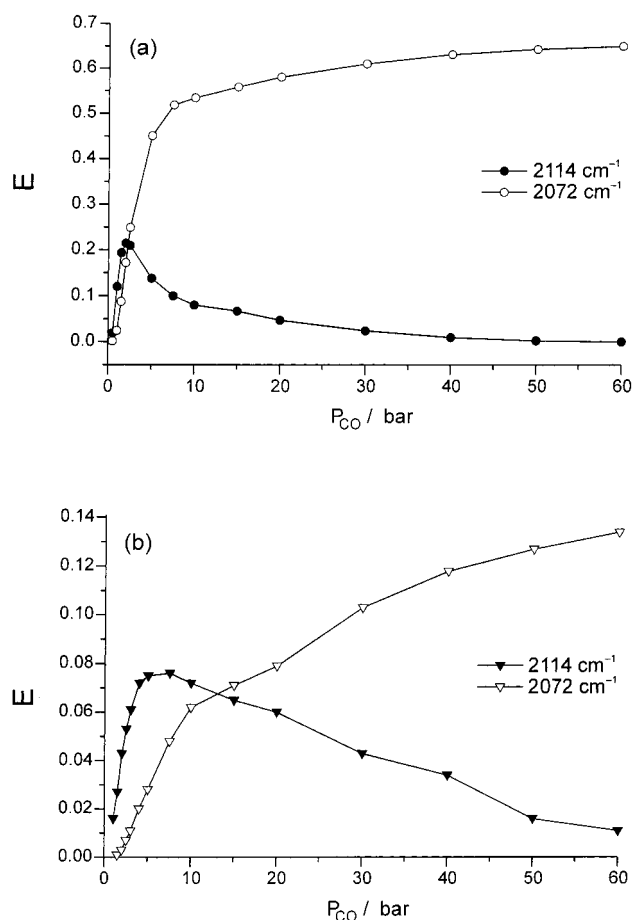


Figure 5. Absorptivities of the bands at 2114 and 2072 cm^{-1} of $\text{Cp}^*_2\text{Yb}/\text{CO}$ in MCH solution at CO pressures from 1 to 60 bar at 20 °C (a, top) and 60 °C (b, bottom).

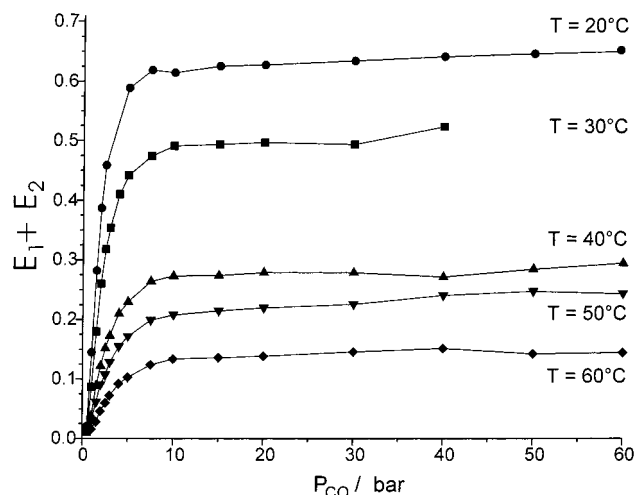


Figure 6. Sum of the absorptivities, $E_1 + E_2$, of $\text{Cp}^*_2\text{Yb}/\text{CO}$ in MCH solutions at 20 °C against CO pressure from 0.5 to 60 bar.

high and low CO pressures, as given in eqs 17 and 18.

$$\text{high } [\text{CO}]: \Sigma E = E_1 + E_2 = A \quad (17)$$

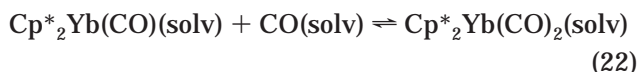
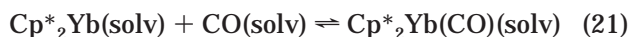
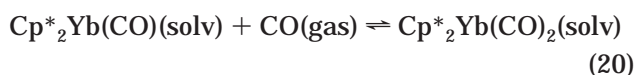
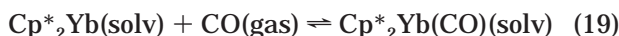
$$\text{low } [\text{CO}]: \Sigma E = E_1 + E_2 = \frac{A[\text{CO}]}{K^{\text{D}}_{\text{C}_1} + [\text{CO}]} \quad (18)$$

Equation 18 yields the values of $K^{\text{D}}_{\text{C}_1}$ for temperatures between 20 and 60 °C by means of Hildebrand-

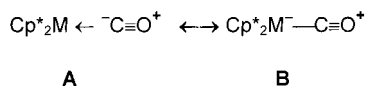
Table 2. Equilibrium Constants K_{C1}^A , K_{C2}^A , K_{P1}^A , and K_{P2}^A for Reaction of Cp^*_2Yb with CO at Temperatures from 20 to 60 °C

temp (°C)	K_{C1}^A (M ⁻¹)	K_{C2}^A (M ⁻¹)	K_{P1}^A (bar ⁻¹)	K_{P2}^A (bar ⁻¹)
20	35(6)	67(3)	0.34(6)	0.66(3)
30	30(5)	36(1)	0.29(4)	0.35(1)
40	28(3)	23(6)	0.28(3)	0.23(1)
50	25(2)	12(3)	0.25(2)	0.12(1)
60	24(3)	8(4)	0.23(3)	0.08(1)

Benesi plots of $1/\Sigma E$ against $[CO]^{-1}$. The corresponding association constants K_{C1}^A are likewise listed in Table 2. Pressure-related association constants K_{P1}^A and K_{P2}^A are derived from K_{C1}^A and K_{C2}^A , respectively, by use of the relation $[CO] = 0.0097P_{CO}$, valid for methylcyclohexane in the temperature range considered.³⁷ Standard enthalpy, entropy, and free energy changes for the association reactions shown in eqs 19–22 can thus be estimated and are listed in Table 1, along with those of K_{C1}^A , K_{C2}^A , K_{P1}^A and K_{P2}^A for 20 °C. The equilibrium constant for the reaction of $Cp^*_2Yb(CO)$ with CO to form $Cp^*_2Yb(CO)_2$ is almost twice that for formation of the monocarbonyl.



The data presented above for CO complex formation with alkaline-earth and bivalent lanthanide metallocenes are to be rationalized in terms of bonding models for complexes of this type. The CO stretching frequencies for the monocarbonyls of Cp^*_2Ca , Cp^*_2Sr , Cp^*_2Sm , and Cp^*_2Eu are increased from that of free CO. The bonding in these monocarbonyls may be rationalized by using a theoretical model proposed some time ago.³⁸ This model implies that when CO is placed in an electrostatic field, with its C atom toward the positive charge, the CO stretching frequency will increase due to coupling between the CO oscillator and this field. This model, which has been used to rationalize the increase of ν_{CO} by about 20 cm⁻¹ when CO binds to metal fluorides in cryogenic matrixes,⁸ as well as to d-transition-metal cations^{39,40} and to solid ZnO,⁴¹ is most likely applicable also to the decamethylmetallocene carbonyl complexes mentioned above. It can be depicted by the valence-bond representations **A** and **B**. These two



(37) Field, L. R.; Wilhelm, E.; Battino, R. *J. Chem. Thermodyn.* **1974**, *237–243*.

(38) Hush, N. S.; Williams, M. L. *J. Mol. Spectrosc.* **1974**, *50*, 349–368.

(39) Goldman, A. S.; Krogh-Jespersen, K. *J. Am. Chem. Soc.* **1996**, *118*, 12159–12166.

(40) Strauss, S. H. *J. Chem. Soc., Dalton Trans.* **2000**, 1–6.

(41) D'Amico, K. L.; McFeely, F. R.; Solomon, E. I. *J. Am. Chem. Soc.* **1983**, *105*, 6380–6383.

representations imply little charge transfer from CO to the electropositive metal fragment, in accord with the slight increase in ν_{CO} and the weak donor–acceptor bonding experimentally observed for these complexes.

The weakness of the M–CO interaction in these complexes will necessarily make them quite susceptible to counteracting interferences and might explain the lack of evidence for any CO complex formation with Cp^*_2Mg and Cp^*_2Ba : in Cp^*_2Mg , the reduced interligand distance will undoubtedly stiffen the metallocene against the bending deformation which is prerequisite for CO uptake.⁴² In Cp^*_2Ba , on the other hand, the rather open Ba center might interact with an aromatic ligand—most likely with the toluene solvent—more strongly than with a CO molecule.⁴³

As mentioned above, the reactions of CO with Cp^*_2Yb are different from those with the other decamethylmetallocenes, since two species are observed in MCH solution, in ratios dependent on the CO pressure. The equilibrium constant for the formation of the monocarbonyl is about an order of magnitude greater for Cp^*_2Yb than that for Cp^*_2Eu and Cp^*_2Ca . The origins of this increased stability of Cp^*_2YbCO are not clear: it must be influenced by such a large number of contributions—most notably the enthalpies and entropies associated with bending the metallocene, with reorganizing its electron distribution, with interligand repulsions, with solvent reorganization, and, finally, with metal–CO bonding—that any partitioning of the experimental ΔH° and ΔS° values into these individual contributions would appear impossible.

Nevertheless, a striking difference is apparent between Cp^*_2YbCO and $Cp^*_2Yb(CO)_2$ on the one hand and all other carbonyl complexes studied on the other hand with respect to the metal–CO bonding, as documented by the opposing direction of the $\nu(CO)$ shifts. To account for the decrease in ν_{CO} in both the mono- and dicarbonyl complexes of Cp^*_2Yb , several bonding models might be advanced: the presence of binuclear species in solution, in which the CO ligand bridges two Cp^*_2Yb fragments, a binding of CO to Cp^*_2Yb either in a side-on fashion or by way of the oxygen atom, and, finally, the classical model of π -back-donation of electron density to an empty π^* -orbital of the CO ligand, bound via its carbon atom, from filled orbitals of Cp^*_2Yb .

Of these possibilities, the last appears the most likely, even though electron density for π -back-bonding from Cp^*_2Yb to CO would have to be derived from the 4f¹⁴ electron population. These are generally considered to represent core electrons in lanthanide metal compounds, which do not participate in metal–ligand bonding except by minor polarization effects.^{44–46} It appears possible,

(42) The structure of Cp^*_2Mg has been found to be linear in the gas phase by electron diffraction studies, while those of Cp^*_2Ca , Cp^*_2Sr , and Cp^*_2Ba were found to be bent: (a) Andersen, R. A.; Blom, R.; Boncella, J. M.; Burns, C. J.; Volden, H. V. *Acta Chem. Scand.* **1987**, *A41*, 24–35. (b) Blom, R.; Faegri, K.; Volden, H. V. *Organometallics* **1990**, *9*, 372–379.

(43) For the tendency of otherwise unshielded Ba(II) centers to coordinate to aromatic C₆ rings see, e.g.: (a) Williams, R. A.; Hanusa, T. P.; Huffman, J. C. *J. Organomet. Chem.* **1992**, *429*, 143–152. (b) Weeber, A.; Harder, S.; Brintzinger, H. H.; Knoll, K. *Organometallics* **2000**, *19*, 1325–1332.

(44) Figgis, B. N. *Introduction to Ligand Fields*; Wiley: New York, 1966; Chapter 13.

(45) Gerloch, M.; Constable, E. C. *Transition Metal Chemistry*; VCH: Weinheim, Germany, 1995.

however, that some 4f-electron density is transmitted to a CO π^* -orbital by way of an admixture of 5d-character to the 4f-orbitals under the influence of the CO ligands. That 5d orbitals might be close enough in energy to the 4f set to rehybridize in Yb(II), but not in Sm(II) or Eu(II) complexes, is supported by the observation that f–d transitions are 7000 cm^{-1} lower in energy for the diethyl ether adduct of Cp^*_2Yb than for the $\text{Cp}^*_2\text{-Eu}$ diethyl ether adduct in the respective photoluminescence spectra in toluene.⁴⁷

This model would also account for other peculiarities of the mono- and dicarbonyl complexes of Cp^*_2Yb . Remarkable in this regard is the observation that $\nu(\text{CO})$ is at lower frequency for the dicarbonyl than for the monocarbonyl species. Normally, for example in chromocene mono- and dicarbonyl complexes,^{29,31} the opposite is observed and is explained by a competition of the CO ligands for metal d-electron density. In $\text{Cp}^*_2\text{-Yb}$ carbonyl complexes, on the other hand, coordination of the first CO ligand appears to achieve only a rather small degree of 5d admixture with the 4f orbitals, which results in a minor red shift of $\nu(\text{CO})$ and in a relatively weak Yb–CO bond,⁴⁸ while coordination of another CO ligand brings about a substantially increased degree of 5d admixture and thus an increased $\nu(\text{CO})$ red shift as well as stronger Yb–CO bonds. Similar ideas have recently been advanced with regard to CO complexes of actinide metal atoms in cryogenic matrices.^{13,14}

While prima facie plausible, even this bond model and its implications for structures and properties of the two Cp^*_2Yb carbonyls is far from being sufficiently substantiated. This is one reason these Cp^*_2Yb adducts are such a fascinating chapter in the organometallic chemistry of the lower valent metallocenes. Further clarification of the interpretations presented above might come from matrix isolation spectroscopy⁴⁹ as well as from in-depth theoretical studies.⁵⁰

(46) Kettle, S. F. A. *Physical Inorganic Chemistry*; Oxford University Press: New York, 1996; Chapter 11.

(47) Thomas, A. C.; Ellis, A. B. *Organometallics* **1985**, *4*, 2223–2225.

(48) The unusually low value of ΔH^\ddagger for the formation of Cp^*_2YbCO results from the small changes in K^\ddagger_{C1} or K^\ddagger_{P1} with temperature (cf. Table 2), which are apparent even from the raw absorbance data; it is thus unlikely to be an artifact generated by the analytical method used.

(49) Perutz, R. N. Personal communication.

(50) Note added in proof: Recent DFT calculations suggest O-bound CO as an alternative in the Cp^*_2Yb case: Maron, L.; Perrin, L.; Eisenstein, O.; Andersen, R. A. *J. Am. Chem. Soc.* **2002**, *124*, 5614–5615.

Experimental Section

All reactions and manipulations were carried out under dry nitrogen or argon using standard Schlenk or drybox techniques. Dry, oxygen-free solvents were employed throughout. Sufficiently dry, oxygen-free methylcyclohexane was obtained only by maintaining the solvent over sodium metal under nitrogen at reflux temperature for at least 1 week; the collected solvent must be used immediately. Insufficient drying or prolonged storage led to some decomposition of the dilute solutions while in the infrared cell. The purity of CO was crucial due to the high pressures used in these experiments. Commercial 99.999% CO was purchased from Messer-Griesheim and passed through an activated oxygen scrubber before use. Use of less pure CO or inattention to experimental detail resulted in decomposition of the sample. The metallocenes were prepared by known synthetic routes: Cp^*_2Mg ,^{42a} $\text{Cp}^*_2\text{-Ca}$,^{42a} Cp^*_2Sr ,⁵¹ Cp^*_2Ba ,⁵¹ Cp^*_2Sm ,⁵² Cp^*_2Eu ,⁵² and Cp^*_2Yb .⁵³ Sample integrity was verified by transferring the cell contents to a Schlenk flask after the infrared measurements and recrystallizing the metallocene. The purity of the metallocene was then tested by measuring its ¹H NMR spectrum or melting point. Another test of sample integrity was comparison of absorptivity before and after an experimental run. The infrared cell was similar to that used previously.²⁷ The gas uptake experiments were performed on a vacuum line of conventional design.³¹

Acknowledgment. This work was partially supported by the Director, Office of Basic Energy Research, Chemical Sciences Division, of the U.S. Department of Energy under Contract No. DE-AC03-765F00098. R.A.A. thanks the Alexander von Humboldt Foundation for a Senior Scientist Research Award, which made visits to the University of Konstanz possible, while M.S. thanks the Alexander von Humboldt Foundation for a postdoctoral fellowship. We also thank Dr. Wayne Lukens for helpful discussions.

Supporting Information Available: A table of equilibrium constants for the reaction of Cp^*_2Ca with CO in toluene at temperatures from -27 to $+32\text{ }^\circ\text{C}$ and figures giving IR spectra of reaction systems containing Cp^*_2Sr , Cp^*_2Sm , and Cp^*_2Eu under CO pressures from 2.5 to 40 bar and a Hildebrandt–Benesi plot for carbonyl complex formation of Cp^*_2Eu . This material is available free of charge via the Internet at <http://pubs.acs.org>.

OM011045R

(51) Burns, C. J.; Andersen, R. A. *J. Organomet. Chem.* **1987**, *325*, 31–37.

(52) Berg, D. J.; Burns, C. J.; Andersen, R. A.; Zalkin, A. *Organometallics* **1989**, *8*, 1865–1870.

(53) Schultz, M.; Burns, C. J.; Schwartz, D. J.; Andersen, R. A. *Organometallics* **2000**, *19*, 781–789.